

Centrifuge Modelling of Driven Piles in Dense Sand

Mr. Davide Bruno

Geomechanics Group, The University of Western Australia, Nedlands, W.A., Australia

SUMMARY

Reliable data on the axial bearing capacity of piles in dense sand is required in order to understand the complex bearing failure mechanisms which occur during pile installation and subsequent loading. The high cost of field testing necessitates that such experimental research is undertaken at model scale, at least initially, allowing fundamental load-displacement behaviour to be investigated. This paper outlines the apparatus and testing regime adopted in the axial loading of driven piles, performed in the geotechnical centrifuge at the University of Western Australia. Typical test results are also presented, which demonstrate the usefulness of the centrifuge as a modelling device for field-scale pile tests.

1. INTRODUCTION

The main reason for the lack of field scale pile test data is due to the high costs associated with such an undertaking. Whilst the extrapolation of centrifuge pile tests to field scale tests (and hence design) is still questionable, the centrifuge remains the principal modelling tool available to researchers in this field.

The centrifuge is ostensibly the only modelling tool that correctly scales the stress gradient due to soil self-weight. This scaling applies to both the free field, and more importantly, to the soil plug within the pile. Centrifuge model tests have a number of advantages over alternative modelling techniques. They allow the accurate reproduction of soil profiles, and permit a wide range of soil and pile parameters to be varied independently.

2. PILE DRIVING APPARATUS

The experimental work presented in this paper was carried out on the fixed beam geotechnical centrifuge facility at the University of Western Australia. The facility houses an Acutronic 661 centrifuge with a capacity of 40 g-tonnes and a platform radius of 1.8 m. A detailed account of the geotechnical centrifuge and associated equipment may be found in Randolph et al., (1).

2.1 Miniature Pile Driving Hammer Actuator

In the centrifuge, the model piles have been installed in-flight using an unique pneumatically operated drop hammer, that simulates a prototype drop-hammer of up to 70 tonnes (ram-mass) such as would be used for an equivalent prototype pile. This piece of equipment has been described in detail by de Nicola, (2) so only the key features are summarised here. A schematic of the moving parts of the actuator is shown in Figure 1. Two double acting pneumatic solenoid valves direct pressurised air into the top and bottom compartments of a piston chamber which forces a piston to pick up the ram mass on its upward trajectory and then allows it to free-fall

under the centrifuge acceleration on its downward trajectory. As a consequence, the hammer impact is correctly modelled.

In addition to permitting in-flight pile installation, the carriage is also capable of pushing or pulling the model pile at low displacement rates. This facilitated the simulation of drained static load testing. The entire carriage can also be displaced through 240 mm vertically and 150 mm horizontally to permit testing at multiple sites if necessary.

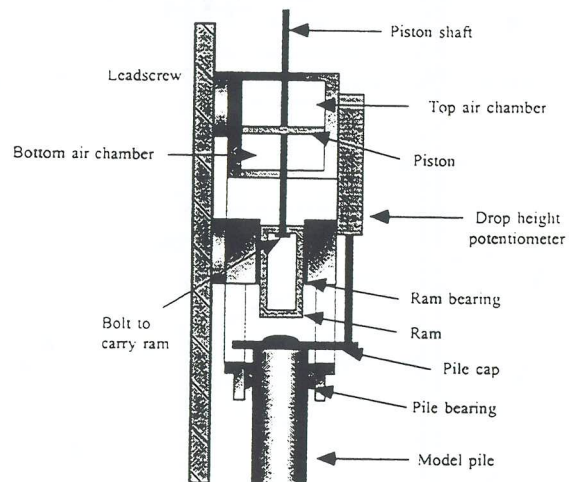


Figure 1 - Working Parts of the Miniature Pile Driving Hammer Carriage

2.2 Model Piles

Figure 2 shows a schematic diagram of the model piles used throughout the centrifuge pile tests. Tests performed with an instrumented pile are denoted IP, and those performed with a less instrumented pile are denoted UP. The instrumented and uninstrumented piles were both fabricated from a thin-walled cylindrical stainless steel section which has had its surface roughened by sand-blasting. In order for the model pile

roughness to correctly scale with the prototype roughness, the ratio of the mean sand particle size, d_{50} and the steel roughness was conserved. By gluing a removable end cap into the toe of the pile a closed-ended pile could also be simulated.

At 100 g the model piles have a prototype diameter, D varying from 0.95 m (UP) to 1.15 m (IP), with a 0.05 m wall thickness and a maximum embedment depth of 20 m.

Varying numbers of strain gauges have been bonded to the model piles in order to measure the axial strain (and hence force) generated during installation and pile loading. In order to protect and seal the gauges from the saturated soil, a thin layer of epoxy resin extends along the shaft of the IP. However, since the volume of soil entering a pipe pile during installation is critically influenced by the ratio of the wall thickness to diameter at the pile toe, the epoxy resin was only extended to the bottom gauge.

The topmost strain gauge was similarly located in both the UP and IP, and remains above the soil surface at all stages of pile installation and testing. This gauge provides a measure of the gross pile behaviour. Additional strain gauges placed along the pile shaft allow the local shaft friction profile along the pile shaft to be determined.

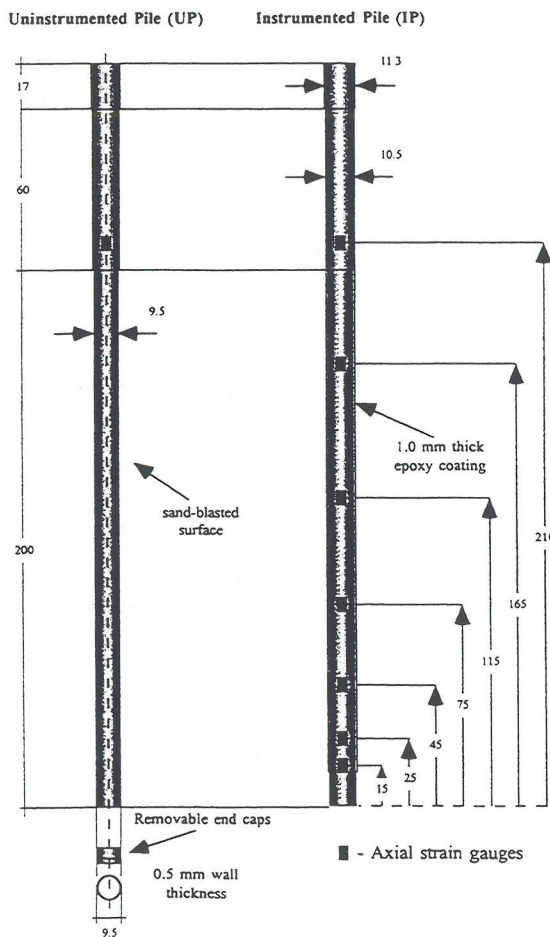


Figure 2 - Model Piles

2.3 Plug Monitoring Device

A displacement transducer is connected to a small 11.9 g aluminium cylinder which is guided along the inside of pile by a high strength kevlar line. The line is passed over pulley housed within the pile cap and attached to displacement transducer, which resides on the actuator. The density of the aluminium cylinder is such that the submerged density is greater than that of water, sufficiently low so that only a light pressure (of around kPa at 100 g) is applied to the internal soil plug.

3. SOIL SAMPLE CONDITIONS

All centrifuge tests were conducted in a saturated fine-grained silica flour (or silt) which has a mean particle size, d_{50} of μm and d_{10} of $9 \mu\text{m}$. The well-graded nature of the soil allows it to be densely compacted, with the potential to attain very high strengths.

Maslen (3) conducted a series of constant normal stiffness direct shear tests on silica flour in order to determine frictional and dilatancy characteristics. Based on tests conducted at varying vertical effective stresses both constant volume friction angles and dilation angles compared very well with those measured for much coarser silica sand. It was concluded that whilst the silica flour had a mean particle size an order of magnitude smaller than a field sand, it correctly modelled the mechanical properties of field scale silica sand.

3.1 Soil Preparation Techniques

Techniques of sample preparation have been refined to a stage where samples with various strength profiles can be prepared. A slurry of silica flour and water was initially mixed and de-aired before being transferred into a test container. After allowing sufficient time for the sample to consolidate, excess water on the surface of the sample was removed, producing a saturated sample with a water content typically around 25%. Varying degrees of soil strength could be achieved by vibro-compacting the sample, which encourages the well-graded silica flour to re-align and compact very tightly. A particular sample density could be achieved by preparing a known mass of saturated silica flour to a given sample height.

3.2 Soil Characterisation

The cone penetration test, (CPT) is a popular and useful characterisation tool used extensively in geotechnical investigation practice. Within the centrifuge the variation of cone tip pressure, q_c with depth was determined using a 7 mm diameter model cone penetrometer. A constant profiling of q_c is obtained during a drained installation of the cone penetrometer into the silica flour. Figure 3 is a plot of q_c with depth for several different centrifuge tests. It can be seen that values of q_c as high as 80 MPa have been measured, which is representative of soil conditions experienced in offshore conditions, particularly in the North Sea.

4. PILE TESTING PROCEDURE

The standard testing container used on the centrifuge is an aluminium segmented box, with internal dimensions 390 mm

wide by 650 mm long and 325 mm high. Up to seven pile tests were conducted along the centreline of any one sample. This ensured that each pile test was separated from the others by a minimum of 7 D. Tests were also a minimum of 13 D and 7 D from the nearest horizontal and vertical boundary respectively. In many instances the separations exceeded these distances.

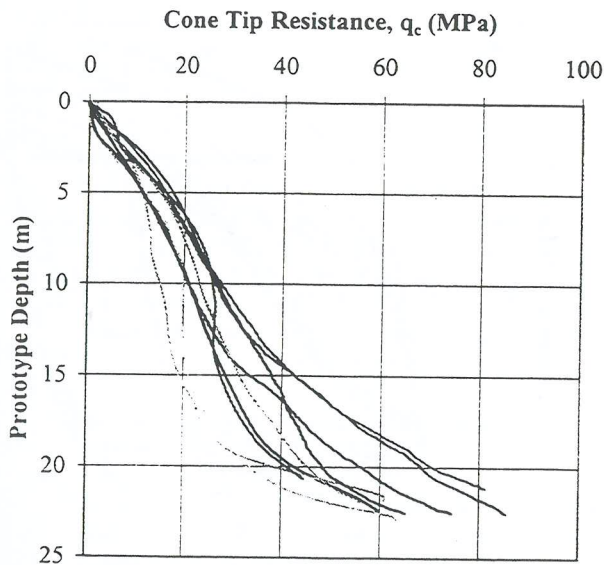


Figure 3 - Cone Penetration Tests

The model piles were installed with the miniature pile driving actuator, which delivered the ram mass with fixed prototype drop heights varying between 1.0 m and 1.7 m. Upon attaining the desired penetration depth, dynamic and static tests were performed on the pile. Dynamic tests involved striking the pile with the ram mass and measuring the transient force and velocity data. Static tests involved driving the entire carriage assembly down (or up) in order to compress (or extend) the pile. Displacement rates used during static tests ensured that drained conditions were maintained throughout the tests. The procedure of driving the pile and then performing static and dynamic tests was repeated at the same testing site for different depths of penetration. Due to the extensive nature of both testing regimes only the static pile tests will be discussed in this paper.

5. PILE TEST RESULTS

5.1 Comparison between IP and UP Static Tests

The size of the instrumentation is relatively large compared to the geometry of the model piles and consequently affects the behaviour of the pile under loading. The first component of the centrifuge testing programme was aimed at quantifying the degree to which the instrumentation affected the loading behaviour. This was achieved by performing identical pile tests using both the UP and IP. The data shown in Figure 4 were derived from a static pile test performed on a pile embedded to a prototype depth of 12.65 metres. The loading path indicated by arrows shows that the compression test

preceded the tension test in both cases. The gross load - displacement behaviour for both the UP and IP is superimposed in order to demonstrate the disparity in magnitude of the prototype pile load at similar pile head displacements.

Traditionally, the static pile capacity is taken at a reference pile head displacement equal to 10 % of the pile diameter (or $w/D = 0.1$). At this reference pile head displacement, the IP mobilised 30 % more soil resistance in compression and 15 % more resistance in tension. The epoxy resin provides an additional 47 % of cross-sectional area and 21 % of surface area to the IP, which perhaps explains why the IP mobilises more soil resistance than the smaller UP. Constant normal stiffness direct shear tests conducted by Maslen, (3) have shown that the interface friction angles of the steel/silica flour and epoxy/silica flour are 29.6° and 31.5° respectively.

A higher frictional angle, in conjunction with greater surface area, would result in higher shaft friction along the IP than the UP.

5.2 Soil Plug Formation During Pile Installation

It is particularly interesting to note the degree to which the instrumentation influenced the formation of the soil plug during installation of the pile. Figure 5 shows the formation of the soil column (or soil plug) for both the UP and IP. The dashed line represents the length of the soil plug if the soil was entering the pile at the same rate as the pile embedment. It is clear that the plug height for both the IP and UP is always less than the embedment depth of the pile. However, the rate of advance of the soil plug in the UP can be seen to approach the rate of pile embedment with increasing pile penetration. In distinct contrast, the rate of advance of the soil plug in the IP is consistently less than the rate of embedment, even though the installation procedures for the UP and IP are similar.

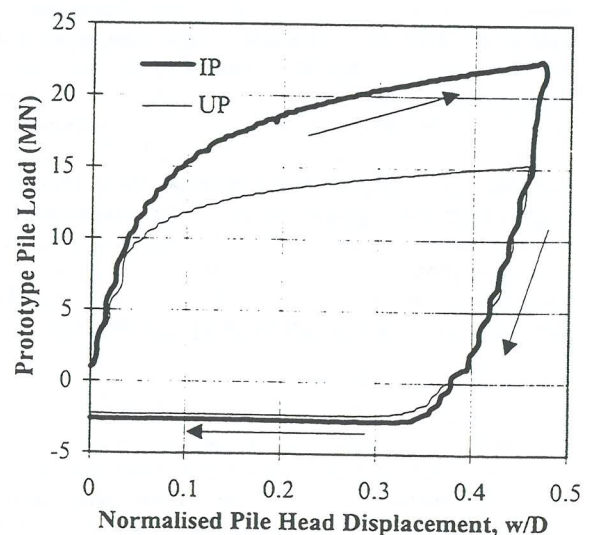


Figure 4 - Typical Pile Static Test

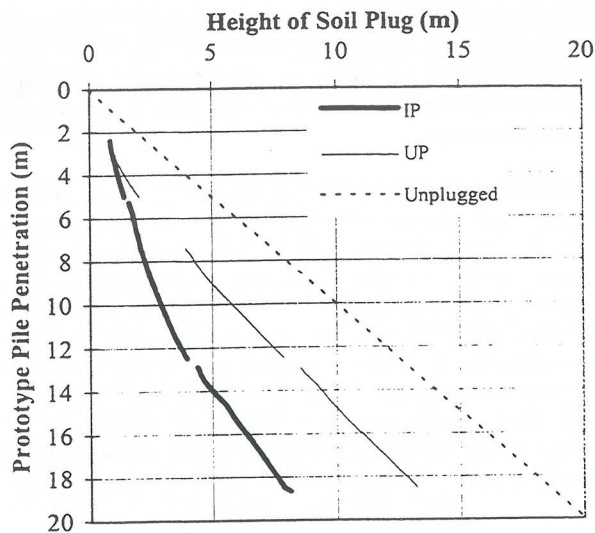


Figure 5 - Formation of the Soil Plug during Pile Installation

This trend was consistently demonstrated by numerous other centrifuge pile tests and suggests that the instrumentation on the IP affects the progression of the plug within the pile, even though it is located a minimum distance of 1.5 D from the pile toe. Perhaps, the larger IP would displace and hence densify a larger volume of soil around the pile tip than the UP. An increase in relative density of the soil would reduce the amount of soil entering the pile toe and consequently reduce the plug height which forms during installation.

It must be noted that while the soil plug continued to form within the open-ended piles during driving, it did not advance during static loading.

5.3 Instrumented Pile

The additional instrumentation located on the IP provides information regarding the distribution of axial load along the length of the pile. The axial load distribution can then be used to calculate more meaningful data such as shaft friction profiles along the embedded portion of the pile, as well as base pressure. In Figure 6, the data from Figure 4 is combined with data generated from the performance of a second static test. The data from all seven gauges are included. As in Figure 4, the topmost curve represents the output from the topmost gauge. The magnitudes of the curves measured by each of the other six gauges reduce with increasing proximity to the pile toe. The outputs of the two gauges near the top of the pile have similar values because they were not embedded during this particular static load test.

5.4 Shaft Friction Profile

In order to estimate the distribution of shaft friction along the pile shaft, the difference in axial load between each gauge has been calculated at a normalised pile head displacement of 0.05. The resultant is then divided by the surface area of the pile between the respective gauges, giving an indication of the local shaft friction acting between the gauges. On the other hand, the local shaft friction acting below the bottom gauge is calculated from the peak value of shaft resistance obtained from gauge 1. A normalised pile head displacement

of 0.05 was generally sufficient to mobilise the peak shaft friction in both compression and tension static tests.

Figure 7 shows the shaft friction profiles deduced from the first compression-tension cycle shown in Figure 6. A close ended static pile test performed at the same penetration depth is included for comparison.

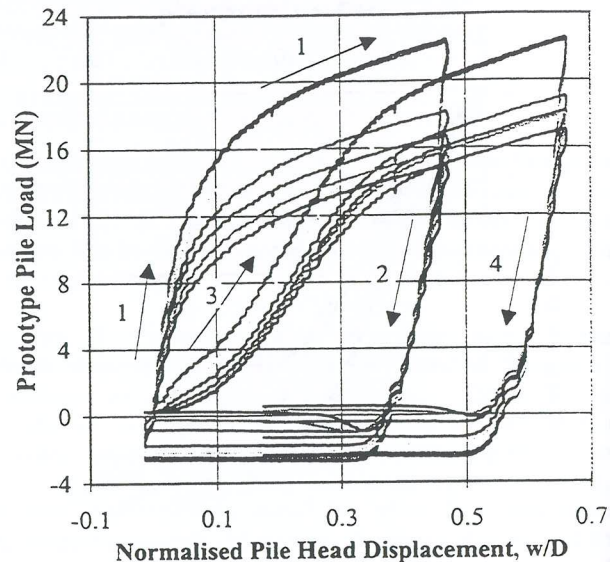


Figure 6 - Typical Static Pile Test (IP)

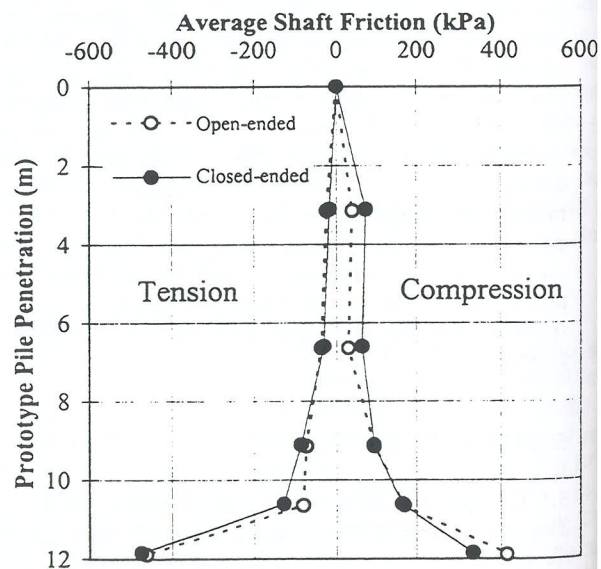


Figure 7 - Typical Shaft Friction Profiles (at a Normalised Pile Head Displacement of 0.05)

A sharp increase in the local shaft friction typically occurs 2-3 D from the pile toe, indicating that most of the shaft

friction was mobilised in this region. In sands, the majority of soil resistance is typically mobilised at the pile toe due to the combination of high end-bearing resistance and high localised shaft friction, which is demonstrated in these centrifuge tests.

A general trend arising from the pile tests is that the closed-ended piles exhibit around 10 % higher average shaft friction compared to the open-ended piles. This can be attributed to greater soil displacement during installation and loading, compared to open-ended piles, which allow the soil to form inside the pile.

5.5 End-Bearing Resistance

The end-bearing resistance can be estimated from the gauge readings closest to the pile toe. An over-estimation of the base pressure, q_b , is made if the axial load, obtained from gauge 1, is simply divided by the cross-sectional area. This includes the contribution of the shaft friction acting below gauge 1, which can cause an overestimation in q_b by up to 10 %.

To overcome this, an alternative approach was implemented. This involved determining the degradation in shaft friction between gauge 2 and gauge 1, and using it to estimate the degradation in shaft friction between gauge 1 and the pile toe. In accounting for the shaft friction mobilised near the pile toe, this approach provided suitably accurate estimates of q_b . Figure 8 shows a typical plot of q_b , which has been normalised against q_c . The cone tip resistance was averaged over a depth of $\pm 1.5 D$ around the pile toe. The normalised base pressure is plotted against the normalised pile toe displacement rather than the pile head displacement. The pile toe displacement can be determined by subtracting the elastic compression of the pile, due to the axial load, from the pile head displacement.

The base capacity of the open-ended pile was less than the closed-ended pile due to elastic compression of the soil plug during static loading. At a normalised pile toe displacement of 0.1 the general trend was for the closed-ended piles to exhibit around 30 % more end bearing resistance than the open-ended piles. However, the increased stress associated with larger pile displacements may be expected to fully compress the soil plug, producing base capacities similar to those of closed-ended piles.

The ratio of q_b/q_c was observed to reduce with increasing overburden stress. The ratio reduced from around 0.6 at a prototype depth of 5 m to as low as 0.18 at 20 m at a normalised pile toe displacement of 0.1. This trend is consistent with tests conducted by de Nicola (2).

6. CONCLUSIONS

The apparatus and testing techniques adopted in the pile tests, conducted at the centrifuge facility at the University of Western Australia, have been outlined. Results from a typical pile test demonstrate the usefulness of the centrifuge as a modelling tool, in as far as plausible results can be readily obtained. The use of instrumented model piles provides qualitatively consistent trends for the mobilisation of shaft friction and end bearing resistance. In addition, the formation

of the soil plug during driving and static loading can also be examined.

However, as with all reduced-scale models, the presence of the instrumentation required to monitor the pile behaviour modifies its behaviour to some degree. Quantifying the effect of instrumentation on the behaviour of model piles is thus central to the correct interpretation of results obtained from any heavily instrumented pile. The need to account for this influence becomes critical when extrapolating to field scale, particularly when postulating new design criteria.

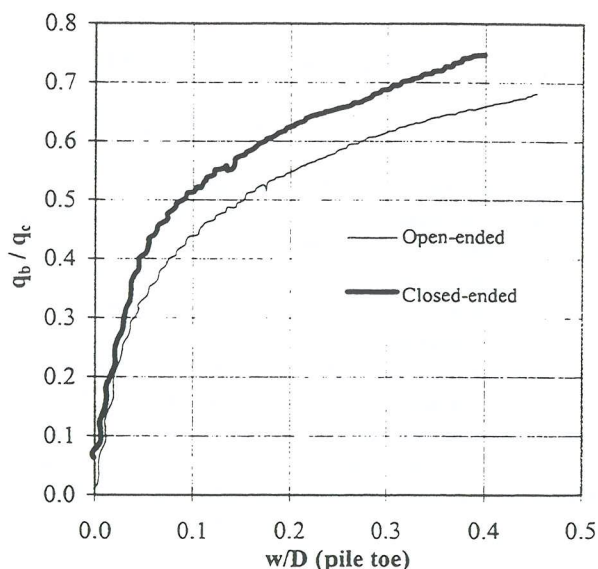


Figure 8 - Base Pressure Normalised with Cone Tip Resistance

7. REFERENCES

1. RANDOLPH, M.F., JEWELL, R.J., STONE, K.J.L. and BROWN, T.A. (1991). "Establishing a new centrifuge facility." *Proc. Int. Conf. on Centrifuge Modeling - Centrifuge 91*, Boulder, Colorado, 39-9.
2. DE NICOLA, A. (1996). "The performance of pipe piles in sand." Ph.D. Thesis, University of Western Australia, Nedlands 6907, Australia.
3. MASLEN, C. J. (1997). "Constant normal stiffness testing of silica sands." Undergraduate Honours Project, University of Western Australia, Nedlands 6907, Australia.